JOURNAL OF HEMATOTHERAPY & STEM CELL RESEARCH 12:255–270 (2003)

Original Research Report

Intravenous Administration of Human Umbilical Cord Blood Cells in a Mouse Model of Amyotrophic Lateral Sclerosis: Distribution, Migration, and Differentiation

SVITLANA GARBUZOVA-DAVIS,[1,2] ALISON E. WILLING,[1–4,6] TANJA ZIGOVA,[1–4] SAMUEL SAPORTA,[1–3] ELEANOR B. JUSTEN, JENNIFER C. LANE, JENNIFER E. HUDSON,[1,2] NING CHEN,[1,2] CYNDY D. DAVIS,[7] and PAUL R. SANBERG[1,2,4–6]

ABSTRACT

Amyotrophic lateral sclerosis (ALS), a multifactorial disease characterized by diffuse motor neuron degeneration, has proven to be a difficult target for stem cell therapy. The primary aim of this study was to determine the long-term effects of intravenous mononuclear human umbilical cord blood cells on disease progression in a well-defined mouse model of ALS. In addition, we rigorously examined the distribution of transplanted cells inside and outside the central nervous system (CNS), migration of transplanted cells to degenerating areas in the brain and spinal cord, and their immunophenotype. Human umbilical cord blood (hUCB) cells (10^6) were delivered intravenously into presymptomatic G93A mice. The major findings in our study were that cord blood transfusion into the systemic circulation of G93A mice delayed disease progression at least 2–3 weeks and increased lifespan of diseased mice. In addition, transplanted cells survived 10–12 weeks after infusion while they entered regions of motor neuron degeneration in the brain and spinal cord. There, the cells migrated into the parenchyma of the brain and spinal cord and expressed neural markers [Nestin, III Beta-Tubulin (TuJ1), and glial fibrillary acidic protein (GFAP)]. Infused cord blood cells were also widely distributed in peripheral organs, mainly the spleen. Transplanted cells also were recovered in the peripheral circulation, possibly providing an additional cell supply. Our results indicate that cord blood may have therapeutic potential in this noninvasive cell-based treatment of ALS by providing cell replacement and protection of motor neurons. Replacement of damaged neurons by progeny of cord blood stem cells is probably not the only mechanism by which hUCB exert their effect, since low numbers of cells expressed neural antigens. Most likely, cord blood efficacy is partially due to neuroprotection by modulation of the autoimmune process.

INTRODUCTION

NEURAL STEM CELL TRANSPLANTATION is a promising therapeutic strategy for treatment of neurodegenerative diseases (1,2), with a goal of replacing lost cells within the CNS or providing support to affected neurons and thereby restoring function. However, in neurodegenerative diseases with complex neural impairment,

[1]Center of Excellence for Aging and Brain Repair, and Departments of [2]Neurosurgery, [3]Anatomy, [4]Pharmacology & Therapeutics, [5]Psychiatry, [6]Pathology, University of South Florida, College of Medicine, Tampa, FL 33612.
[7]Saneron CCEL Therapeutics, Inc., USF Center for Entrepreneurship, Temple Terrace, FL 33617.

such as amyotrophic lateral sclerosis (ALS), this transplantation has not been considered a viable therapeutic option.

In agreement with Bruijn's (3) comment concerning neural stem cell replacement therapies for ALS, "it is hard to imagine that transplanted motor neurons would form appropriate connection with target muscle," there are severe limitations to using this treatment in ALS. First, ALS is characterized by rapid and diffuse degeneration of motor neurons in the spinal cord, motor cortex, and some brainstem nuclei that clinically manifests as a progressive muscular weakness leading to paralysis and death. Early diagnosis is difficult because initial degeneration may be more localized. The advanced stage of disease at diagnosis and the multiple transplantation "targets" may limit this treatment approach. However, a local effect by neural transplantation can be attained. Recently, our studies in a G93A transgenic mouse model of ALS showed that symptom onset and disease progression were postponed when hNT neurons (neurons derived from a human teratocarcinoma cell line) were transplanted into the spinal cord of both nonsymptomatic mice and mice with apparent motor deficit (4–6). Secondly, the etiopathology of ALS includes oxidative stress and glutamate excitoxicity (7,8), mutations in the gene for Cu/Zn superoxide dismutase (9), viral infection (10), autoimmune mechanisms (11–13), abnormal accumulations of neurofilaments (14,15), altered glial function (16–19), mitochondrial dysfunction (20,21), and possible impairment of trophic support (19). Due to the multiple interdependent factors underlying the pathogenesis of this disease, it is difficult to envision that pathological changes are postponed merely by replacement or restoration of the motor neurons. More likely, transplanted stem cells of nonneuronal origin have additional mechanisms preventing degeneration of nearby motor neurons in the host environment.

Stem cells from human umbilical cord blood (hUCB) may be preferable to either bone marrow or neural stem cells as a source of cells for transplantation because hUCB cells are of nonfetal origin, easy to obtain, available for collection after delivery, and remain viable after long-term cryopreservation. Although hUCB contains a heterogeneous cell population, it is relatively rich in hematopoietic stem and progenitor cells (22,23) that appear to have an unusual capacity to develop into a nonhematopoietic cell type. *In vitro* studies conducted by our research group have shown that these cells can differentiate into neural phenotypes expressing molecular neuronal/glial markers, after exposure to retinoic acid and nerve growth factor (RA + NGF) (24,25). These results have been verified by other researchers (26,27). The hUCB cells have since been transplanted into the neonatal rat brain, to explore further their survival and phenotypic properties. When the hUCB cells were transplanted into the anterior subventricular zone (SVZ), approximately 20% of transplanted cells survived (without immunosuppression) within the neonatal brain, and were observed in the SVZ, striatum, corpus callosum, and cortex (28). Some of these cells expressed neuronal (TuJ1) and glial markers [glial fibrillary acidic protein (GFAP)] after being exposed to instructive signals from the developing brain. Moreover, intravenously transplanted hUCB cells in animal models of stroke, spinal cord, or brain injury can migrate to regions of degeneration and reduce behavioral deficits (29–31). In an ALS mouse model, intravenous administration of hUCB (35×10^6 cells) substantially increased the lifespan of mice (32,33). The hUCB cells were transplanted into irradiated mice and the authors (32) suggest that these cells may possibly "provide enhanced hematopoietic reconstitution of the irradiated hosts own stem cells." While the survival data was impressive, the investigators did not examine motor function in these animals or determine the underlying mechanism(s).

Together, these results suggest that hUCB may have therapeutic potential for repair of the injured nervous system, even one with such extensive damage as in ALS. However, it is unclear whether this cell therapy acts by providing cell replacement, neurotrophic/neuroprotective support of dying motor neurons in ALS, or some combination of these actions. We hypothesize that the hUCB cells will have a combinatory (cell replacement and neuroprotection) effect in the treatment of ALS. Additionally, the delivery route of transplanted cells is key for this multifocal neuronal injury as well as for developing a novel, noninvasive therapy easily accessed by ALS patients.

The primary aim of this study was to determine long-term effects of intravenous mononuclear hUCB cell administration upon disease progression in a mouse model of familial ALS. The secondary aims were to investigate the distribution of transplanted hUCB cells inside and outside the CNS, and their possible migration to areas of degeneration in the brain and spinal cord and to determine their immunophenotype(s). Results of these investigations will advance our understanding of the transplant effects and the risk/benefit ratio of hUCB transplants as a treatment for ALS.

MATERIALS AND METHODS

Animals

Transgenic male mice B6SJL-TgN (SOD1-G93A) 1GUR (G93A; obtained from Jackson Laboratories, Bar Harbor, MA), overexpressing human SOD1, carrying the Gly_{93} Ala mutation (34), were used. Mice randomly received hUCB cells into the jugular vein (hUCB jv, $n = 9$) or Media (Media jv, $n = 10$) at 66.2 ± 0.75 days (9.5

weeks) of age. Independent investigators were blinded to the animal's post-transplant status to avoid subjective bias. The blinding code was revealed when the last animal was perfused. All mice were maintained on a 12:12 h dark:light cycle (light on at 06:00 h). Room temperature was 23°C. Food and water were available ad libitum.

Preparation of hUCB cells for transplantation

The hUCB cells from unrelated donors were donated for research purposes by a cord cell blood bank. Cryopreserved hUCB cells (Saneron CCEL Therapeutics Inc., Tampa, FL) were thawed rapidly at 37°C and then transferred slowly with a pipette into a 15-ml centrifuge tube containing Isolyte S, pH 7.4 (BBraun/McGaw Pharmaceuticals). The cells were centrifuged (1000 rpm/7 min), the supernatant discarded, and the process repeated. After the final wash, viability of cells was assessed using the 0.4% Trypan Blue dye exclusion method prior to and following transplantation. The cell concentration for each transplant was adjusted to 100,000 cells/μl.

Surgery

The hUCB cells were delivered intravenously. The jugular vein was exposed and isolated using blunt dissection. The vein was ligated and a small hole made with a 26-gauge needle. A 31-gauge needle, attached to a 10-μl Hamilton syringe, was placed into the lumen of the vein and sutured in place. The cells (100,000 cells/μl, 10^6) or Media (Isolyte S, pH 7.4) were delivered during 5 min. The needle was withdrawn, the suture tightened, and the incision closed. All animals were immunosuppressed with cyclosporine (10 mg/kg i.p. per day) during the post-transplantation period.

Characteristics of disease progression

The evaluation of animal disease progression was previously described (4–6). Animal testing was performed blinded. Briefly, the body weight was measured weekly throughout the study. Extension reflex and footprints were observed 1 week prior to transplant, at 12, 14, and 16 weeks of age, and then weekly.

Extension Reflex: The mouse was suspended by its tail and extension of hindlimbs observed. A score (0–2) was given to each mouse indicating: normal (2), partial (1), or absent (0) hindlimb extension.

Footprint: The mouse left a series of footprints on a paper track (50 × 10 cm). Run time and number of steps were measured.

Statistics: Data are presented as means ± SEM. The nonparametric Kruskall Wallis H test was used to compare medians. Post hoc testing used either Dunn's Multiple Comparison procedure (equal n's) or Newman-Keuls Multiple Comparisons procedure (unequal n's). The results of footprint analysis were evaluated using the unpaired Student's *t*-test. The Kaplan-Meier method was used to determine the difference in survival rate between the groups of hUCB transplanted or Media-injected mice and is reported as a chi-square value (χ^2).

Morphological characteristics of cultured living cells

Cryopreserved hUCB cells were plated on poly-L-lysine-coated (10 μg/ml, Sigma) eight-well chamber slides at a concentration of 100,000 cells/cm^2, and cultured in Dulbecco's modified Eagle's medium (DMEM, Gibco) with 10% fetal bovine serum (FBS, Gibco) and gentamicin (50 μg/ml, Sigma). The morphology of living hUCB cells was observed at 2, 24, and 48 h, 7 days (days in vitro, DIV), and 5 weeks after plating.

Immunocytochemistry of hUCB cells in vitro and in vivo

Most of the antibodies used to identify the immunophenotype of the hUCB cells were mouse monoclonal antibodies and the transplants were conducted in mice, so *in vitro* characterization of hUCB cells was performed first. For immunocytochemistry, the cultures were fixed (4% paraformaldehyde) after 1 h, 24 h, 7 and 14 DIV.

In vitro: Two protocols were used to validate the labeling of hUCB cells with human-specific antibody. In the standard immunostaining protocol, cells from the short-term (24 h) culture were stained overnight with mouse monoclonal antibody against human nuclei (HuNu, 1:50, Chemicon) followed by 2 h of incubation in secondary antibody fluorescein isothiocyanate (FITC)-conjugated goat anti-mouse (1:500, Alexa Molecular Probes). The other procedure was adapted from Mason et al. (35) and has been previously described (4,5). Briefly, the mouse monoclonal antibody (HuNu, 1:50, Chemicon) was combined with the secondary antibody, monovalent goat anti mouse Fab′ fragment conjugated to FITC (1:200), prior to tissue application. This antibody cocktail, which had been previously incubated for 2 h at room temperature, was applied on the tissue. After incubating overnight at 4°C, the slides were rinsed in phosphate-buffered saline (PBS) and coverslipped with DAPI.

To determine the expression of specific phenotypical immunomarkers, the cells were immunostained overnight with mouse monoclonal anti-human antibodies for CD (Cluster Designation) antigen expression: CD133 (1:50, Miltenyi Biotec), CD34 (1:50, Santa Cruz Biotech), CD45 (1:700, BD Biosci), CD11b (1:200, Serotec); Nestin (1:100, BD Trans lab); β-tubulin III (TuJ1, 1:500, Covance) or with rabbit polyclonal antibodies against

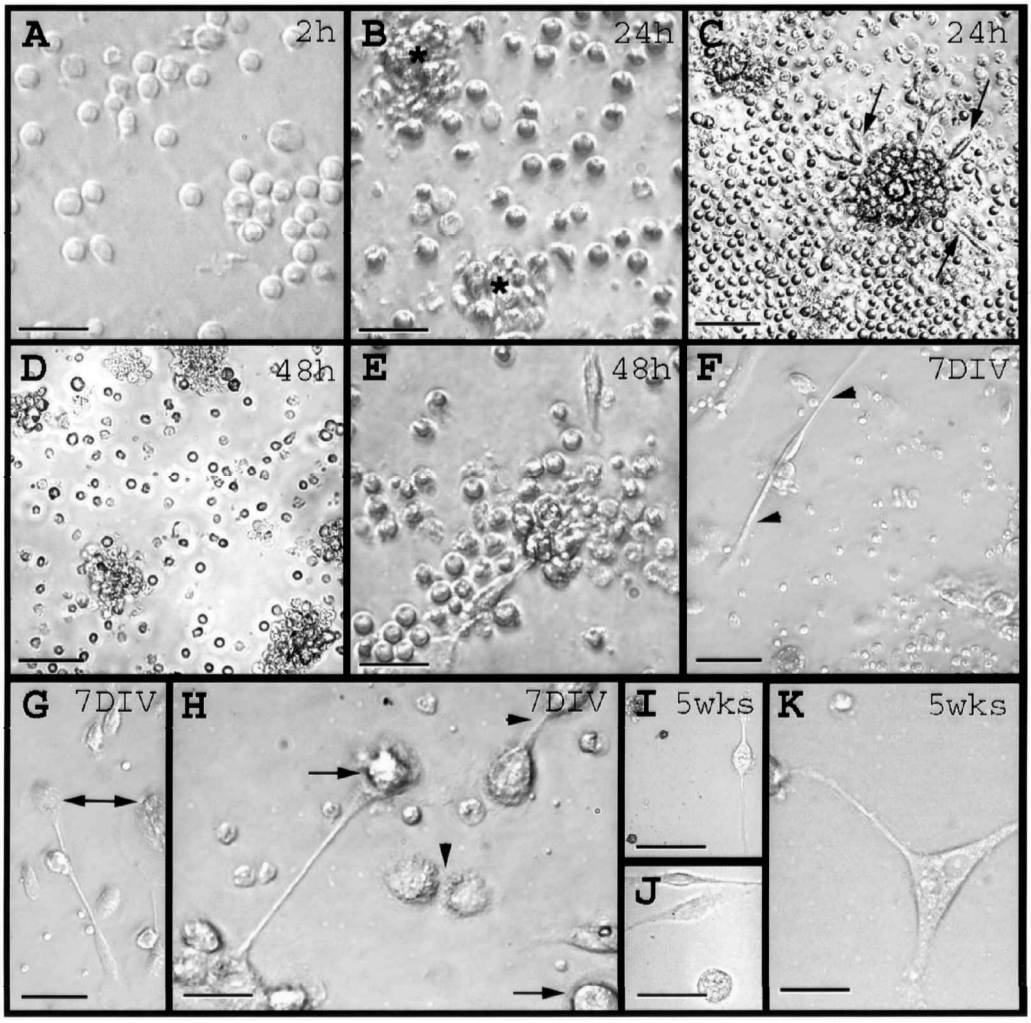

FIG. 1. Phase-contrast images of living hUCB cells at 2 h to 5 weeks after plating in DMEM and 10% FBS. (**A**) A monolayer of homogenous round cells appeared 2 h after plating. (**B**) After 24 h, occasional clusters (*stars*) of small cells were noted. (**C**) In some instances, individual cells (*arrows*) were leaving the cluster. (**D**) The number of cluster formations was significantly higher after 48 h. (**E**) Spindle-shaped cells were frequently found throughout the culture dish. After 7 days *in vitro* (7DIV), many cells with long bipolar processes (*arrowheads*) surrounded by small, round (probably proliferating) cells (**F**) and large round cells with prominent nuclei (*arrows*) were observed (**G,H**). Cell division was also apparent (**H**, *arrowheads*). (**I–K**) During the longest culture period (5 weeks), many cells developed neuron- and glial-like morphology, atypical for hematopoietic cells. Scale bar: in C, D, F, and G, 50 μm; A, B, E, H, I, J, and K, 25 μm.

FIG. 2. Human umbilical cord blood cells express human-, cluster designation (CD), and neural-specific antigens *in vitro*. Panel (**A**) Immunohistochemistry for human specific markers. Parts A–C. After 24 h of plating, all cultured hUCB cells were immunopositive for human nuclei using the standard or our modified protocol (parts D–G). There were no differences between the two protocols in staining of cell nuclei (*arrowhead*) and cell cytoplasm (*arrow*). The nuclei in parts a–g are shown stained with DAPI. Scale bar: parts A and B, 20 μm; parts C–G, 10 μm. Panel (**B**) Immunohistochemistry for CD antigen expression. (Part A) A few cells were immunopositive for CD34 (red/orange, *arrow*) and CD133 (green, *arrow*), 1 h after plating. (Part B) Most cells expressed CD45 (red/orange, *arrow*) and only a few cells were positive for CD11b (green, *arrow*), 1 h after plating. (Part C) Many more small cells expressing CD133 (green, *arrow*) appeared at 7 days than at 1 h after plating. (Part D) Double-staining for CD45 (red/orange) and CD11b (green, *arrow*) after 7 days *in vitro*. The nuclei in parts a–d are shown with DAPI. Scale bar, parts A–d, 20 μm. Panel (**C**) Immunohistochemistry for neural-specific markers 2 weeks after plating. (Part A) Nestin-positive (red, *arrow*) and Nestin-negative cells (*arrowhead*). (Part B) Double-labeled cells expressing Nestin (orange, *arrow*) and MAP2 (green, *arrow*). (Part C) Control staining for Nestin and MAP2 (primary antibodies are absent). (Parts D and E) Merged images of GFAP-labeled hUCB cells (green) with DAPI counterlabeled nuclei (blue). *Arrowhead* indicates GFAP-negative hUCB-derived cell. (Parts F–H) Various cytoplasmic localizations of TuJ1 antigen (red, *arrow*) were observed in cells with different morphology. TuJ1-negative cells were verified by DAPI staining (*arrowheads*). Merged images. Scale bar, parts A–H, 25 μm.

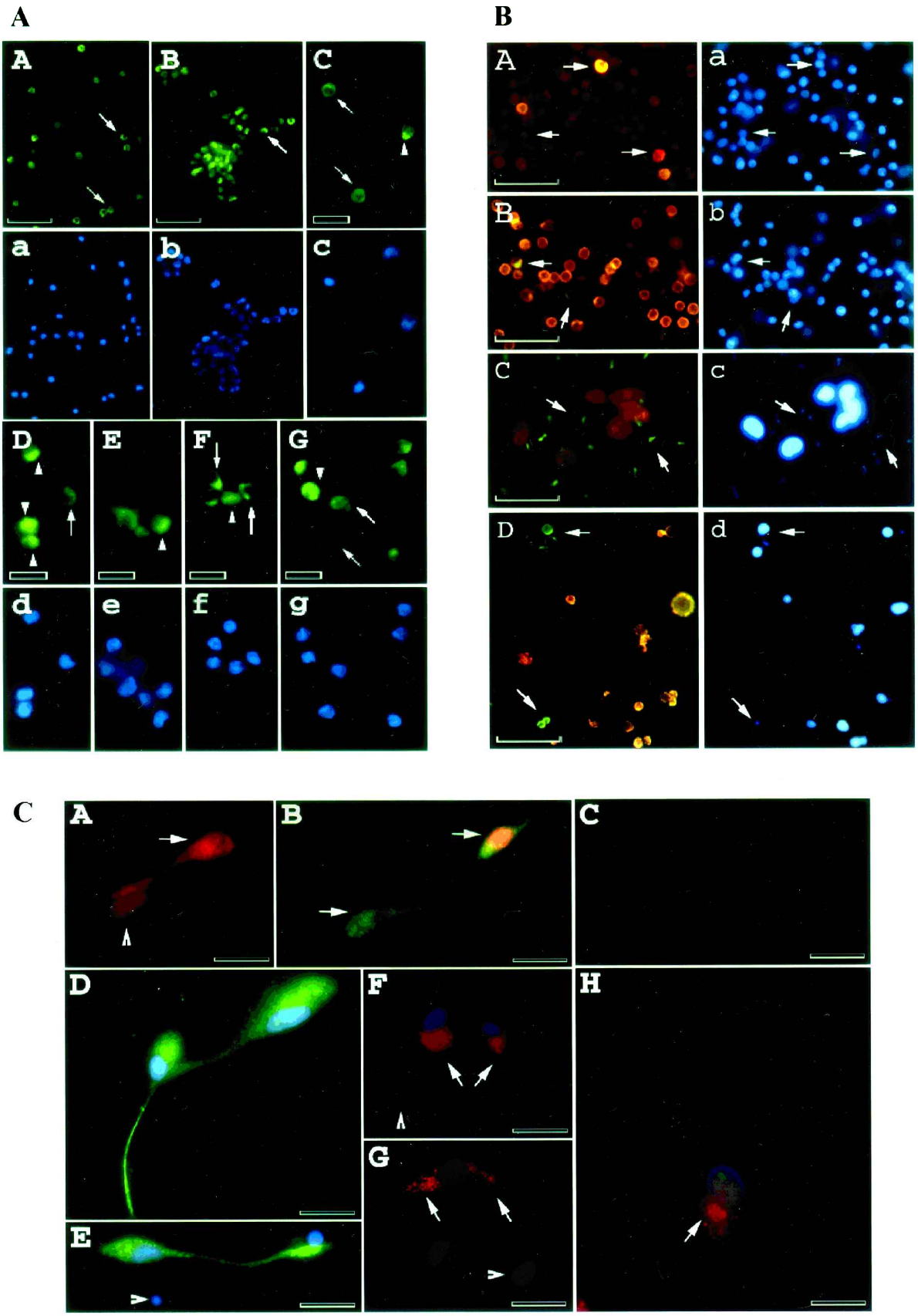

FIG. 2.

GFAP (1:600, Dako) and microtubule-associated protein 2 (MAP2, 1:1,000, Chemicon). Some cultures were stained with the antibody cocktail for Nestin and MAP2. The next day, the slides were incubated with appropriate secondary antibodies conjugated to either rhodamine or fluorescein (1:500–700, Alexa, Molecular Probes) for 2 h at room temperature and then rinsed several times in PBS. All culture slides were coverslipped with Vectashield (Vector) or Vectashield with DAPI (Vector) and viewed with an Olympus BX-60 microscope through rhodamine, fluorescein, or DAPI filters. Co-localization of two immunomarkers on cells was visualized through a double-filter.

In vivo: When the progression of disease symptoms reached the point of paralysis, mice were sacrificed under deep chloral hydrate (10%) anesthesia and perfused transcardially with 4% paraformaldehyde in 0.1 M phosphate buffer, pH 7.2. The brain, cervical and lumbar spinal cord, and the organs (heart, lungs, liver, spleen, and kidneys) of intravenously transplanted mice were removed, post-fixed, and then cryoprotected in 20% sucrose in 0.1 M phosphate buffer, pH 7.2, overnight. Coronal, horizontal, or sagittal sections were cut at 30 μm in a cryostat.

Serial sections of the brain, spinal cord, and organs were thaw-mounted on slides, washed with deionized water to remove the freezing medium, and then rinsed several times in PBS. The tissue was then placed in 1% normal human serum (NhuS) in PBS, 0.5% Triton 100X for 30 min at room temperature. For identification of the hUCB within mouse tissues, the initial basic immunostaining with HuNu antibody cocktail was performed as described above. Then, after several rinses in PBS, the sections of the brain and spinal cord were double-stained with mouse monoclonal antibodies for CD45 (1:500), Nestin (1:100), TuJ1 (1:500), or rabbit polyclonal antibodies for GFAP (1:600). The organ tissues, after staining with HuNu, were then stained with antibodies for CD45 (1:500) or CD34 (1:50). The next day, the slides were incubated with appropriate secondary antibodies conjugated to rhodamine (1:500–700, Alexa, Molecular Probes) and, after several rinses in PBS, coverslipped with Vectashield or Vectashield with DAPI and examined under epifluorescence.

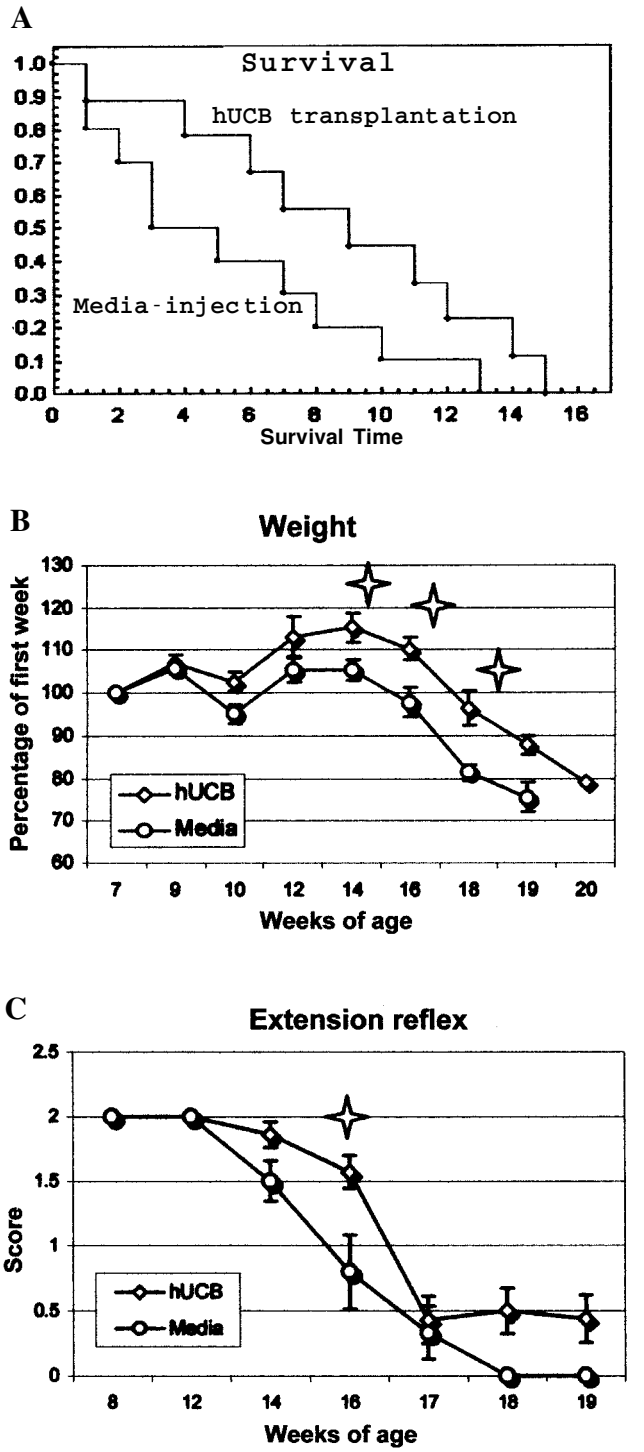

FIG. 3. Characteristics of disease progression in hUCB transplanted and Media-injected G93A mice. (**A**) Kaplan-Meier survival curves for mice; days of age: (2) 70–72, (4) 77–101, (6) 119–123, (8) 124–125, (10) 128–133, (12) 134–135, (14) 137–139, and (15) 144. The administration of hUCB cells or Media was at 66.2 ± 0.75 days of age. (**B**) Graphs of body weight and (**C**) extension reflex of G93A mice with hUCB administration (hUCB) and Media-injection (Media). The four pointed star in **B** and **C** indicates significant differences between two groups ($p < 0.05$).

RESULTS

Immunophenotypical characterization of hUCB cells in vitro

When hUCB cells were plated in Dulbecco's modified Eagle medium (DMEM) with 10% fetal bovine serum (FBS), homogenous round cells formed clusters after 24 h. After 48 h, the number of cluster formations was sig-

nificantly greater and spindle-shaped cells were frequently found. Seven days after plating, many cells with long bipolar processes surrounded by small, round (probably proliferating) cells and large round cells with prominent nuclei were observed. Cell division was also apparent. In long-term culture (5 weeks), cells developed heterogeneous morphological characteristics; many cells had a neuron- and glial-like morphology, atypical for hematopoietic-derived cells (Fig. 1).

Using human-specific antibody as a marker for hUCB cells in either the standard or our modified protocol, all cells after 24 h of plating were immunopositive for human nuclei. There were no differences between the two protocols in staining of cell nuclei and cell cytoplasm. However, most cells expressed this marker in their cytoplasm (Fig. 2, parts A–D, F, G; panel A).

The examination of hematopoietic cell-surface antigen (CDs) expression was performed at 1 h and at 7 DIV on hUCB cells. One hour after plating, some of these cells expressed CD34 (hematopoietic progenitor/stem cell marker), CD133 (primitive progenitor/stem cell marker), and CD11b (macrophage marker), but most expressed CD45, the common leukocyte antigen. Interestingly, at 7 DIV, there appeared to be more $CD133^{+}$ cells than at 1 h. The other examined antigens (CD34, CD45, and CD11b) were still present at this time (Fig. 2B, panel B).

In long-term culture (2 weeks), when cells were demonstrating distinct morphologies unusual for hematopoietic cell lineages, some cells expressed specific markers, indicating early neural (Nestin), early (TuJ1) and mature (MAP2) neuronal, as well as astrocytic (GFAP) antigens (Fig. 2, panel C). These, and other neural markers expressed by hUCB cells, were observed in the early studies of our research group (24,25).

Thus, our *in vitro* results demonstrate that there is a heterogeneous population of hUCB cells that exhibit hematopoietic and neural-like phenotypes. New findings in the present study were the co-localization of Nestin and MAP2 in cells and nonconventional cytoplasmic localizations of TuJ1 protein.

Effect of hUCB cell administration on disease progression

When hUCB cells (10^6) were administered intravenously into G93A mice at 9 weeks of age, the increase in survival between transplanted and Media-injected groups approached significance ($\chi^2 = 2.618, p = 0.10$; Fig. 3A). Average lifespan of hUCB-administered mice was 17.4 ± 1.17 weeks compared to 14.3 ± 1.39 weeks of Media mice, with post-transplant survival of 57 ± 8.42 and 33.2 ± 9.61 days, respectively. Some animals (44%) from the hUCB group were alive until 19–21 weeks of age, whereas Media-injected mice survived no longer than 17–19 weeks of age.

At 13–14 weeks of age, symptoms of disease progression appeared in the experimental G93A mice. The 14 weeks of age, Media-injected mice started to lose weight ($\chi = 6.017$, $p = 0.0142$) while hUCB-transplanted animals maintained body weight until 16 weeks of age ($\chi = 8.3449$, $p = 0.0394$), after which time weight began to slowly decrease. These hUCB mice at 18 ($\chi = 5.5451, p = 0.0185$) and 19 weeks of age showed losses of 4% and 12% in body weight, respectively, while Media mice at these times lost about 19% and 24.5% of their pretransplant weight (Fig. 3B).

Thirteen weeks of age was a critical time, when Media-injected animals started a sharp deterioration in extension reflex (Fig. 3C). The hUCB-transplanted mice showed significantly more instances of hindlimb extension at 16 weeks of age ($\chi = 4.8066$, $p = 0.0284$) and demonstrated hindlimb extension until 19 weeks of age (Fig. 3C). By 18 weeks of age, Media animals had no extension and exhibited hindlimb paralysis. It is interesting to note that tremor, an initial sign of disease, was subtle in the hUCB mice.

In the footprint test, motor deficit of Media mice was observed as early as 13 weeks of age (Table 1). Although

Table 1. Footprint Characteristics of G93A Mice after hUCB Administration or Media Injection

		Weeks of age				
Parameter	*Groups*	*8*	*13*	*15*	*17*	*19*
time (sec)	hUCB	3.1 ± 0.62	1.9 ± 0.32	5.1 ± 1.17	14.8 ± 3.29*	48.8 ± 9.53
	Media	4.0 ± 0.54	2.8 ± 1.25	5.3 ± 2.72	57.3 ± 20.48	
step (no.)	hUCB	12.9 ± 0.69	13.8 ± 0.52	15.1 ± 1.23	24.7 ± 2.39	46.3 ± 7.43
	Media	15.3 ± 0.55	13.6 ± 2.31	15.5 ± 0.75	25.5 ± 3.24	

Note: Time and number of steps were counted for a series of footprints on a paper track (50 × 10 cm). Media-injected mice at 17 weeks of age did not complete the 50-cm run due to dragging or paralysis of the hindlimbs. Comparison of step numbers at 17 weeks is thus misleading.

*Significant ($p < 0.05$) differences between two groups.

there were no significant differences between hUCB and Media groups in number of steps at this time, Media-injected animals averaged longer run times (2.8 sec) compared to hUCB mice (1.9 sec). One month later, at 17 weeks of age, major footprint changes were also found in the Media-injected mice. The travel time of these mice was four times longer (57 sec) than that of the hUCB transplanted animals (15 sec) ($t = -3.1549$, $p = 0.0116$). Most Media mice were not able to complete the run on a paper track due to dragging of both hindlimbs. (The similar step numbers between the two groups at 17 weeks is misleading, reflecting the incomplete runs of the Media mice). The hUCB mice tested at this time (17 weeks of age) exhibited partial dysfunction of their hindlimbs but could perform this test until 19 weeks of age.

Thus, the intravenous administration of hUCB cells into G93A mice may delay progression of disease for at least 2–3 weeks. Although no mice receiving the cells lived longer then 21 weeks of age, their survival rate was higher than Media-injected mice. Compared to Media-injected mice, hUCB-transplanted mice showed superior motor function, manifested by only slight decreases in body weight and the retention of some movement ability, with partial hindlimb function observed until late-stage disease.

Distribution and immunophenotype of transplanted hUCB cells

Characteristics of hUCB cells outside the CNS: Ten to twelve weeks after jugular vein transplant, many hUCB cells were found in the blood vessels and parenchyma of organs: spleen, kidneys, liver, lungs, and heart (organs listed in decreasing order of cell density by our subjective estimate). Most cells were immunostained only with HuNu; some expressed CD45 or CD34 antigens.

In the heart, the hUCB cells were found in blood vessels (Fig. 4A, panel A). A few cells, identified between myofibers, expressed only anti-human antigen (HuNu) and showed an unusual morphology for hematopoietic cells, (Fig. 4B, panel A). Some transplanted cells were found in capillaries between connective tissues and were double-labeled for HuNu and CD45 (Fig. 4C, panel A). All hUCB cells in the heart were negative for CD34.

The hUCB cells in the lungs were also localized in blood vessels of various calibers surrounding the alveolar sac (Fig. 4D, panel A). There were no cells expressing either CD45 or CD34 and their morphology appeared similar to that of epithelial cells.

Many transplanted cells were found between hepatocytes or in the sinusoids of the liver. A number of these cells shared a similar appearance with Kupffer cells (Fig. 4E–G, panel A). Although some cells expressed either CD45 or CD34 antigens, some were negative for both of these markers.

We noted that many transplanted hUCB cells were present in the cortex and medulla of the kidneys, in containing and collecting tubules, respectively. Transplanted cells located between the tubules showed endothelial-like cell morphology and expressed CD45 antigens. Some $CD34^+$ cells were identified within the tubules (Fig. 4H–J, panel A).

In the spleen, the majority of hUCB cells were identified in the white pulp (Fig. 4A, panel B). Transplanted cells in the lymphoid nodules were mostly positive for CD34 and less so for CD45 (Fig. 4B–D, panel B). Interestingly, some hUCB cells did not express either CD marker, being positive only for HuNu.

Thus, 10–12 weeks after intravenous administration of hUCB cells into G93A mice, the cells were found widely distributed in all examined organs of the body. Although many cells were associated with blood vessels, confirming that transplanted cells were still present in the blood circulation, some cells were found in the parenchyma. This intraparenchymal migration of hUCB cells in some organs was indicated by cell type morphologies specific to the individual organs.

Characteristics of hUCB cells found within the CNS: Immunocytochemically, the hUCB cells identified by the human-specific marker (HuNu) were widely distributed

FIG. 4. Distribution and hematopoietic immunophenotype of intravenously administered hUCB cells in peripheral organs. Panel (**A**). (Part A) The cells are found in the blood vessels of the myocardium in the heart and (part B) between myofibers (green). (Part C) Some cells are double-labeled for CD45 and HuNu (*orange, arrows*) or only express HuNu *(green, arrowhead).* (Part D) HuNu-positive cells in lung blood vessel (*green*) reveal morphology similar to that of epithelial cells. (Parts E and F) In the liver, hUCB cells co-expressing HuNu and CD45 (*green/red, arrow*) have morphology of Kupffer cells; some are negative for CD45 (*green, arrowheads*). (Part G) Co-localization of HuNu and CD34 (*green/red, arrow*) in the liver; many of these cells are found in containing (part H, *green*) and collecting tubules of the kidneys. (Part I) Some cells co-express HuNu and CD45 markers (*green/red, arrow*) and show endothelial-like morphology (*green, arrowhead*). (Part J) Double-staining for HuNu and CD34 reveals immunoreactive hUCB cells within the tubules (*orange, arrow*). Scale bar: A–G, I and J, 25 μm; H, 100 μm. Panel (**B**). (Part A) Many hUCB cells found in the white pulps of the spleen express CD45 (part B) and CD34 (parts C and D). These double-stained cells are indicated by arrows in parts B, C, and D with *green* immunofluorescence for HuNu surrounded by *red* immunolabeling for CD antigens. Arrowheads in parts C and D show negative staining for CD34 (*green*). WP, White pulp; RP, red pulp. Scale bar: A, 50 μm; B–D, 25 μm.

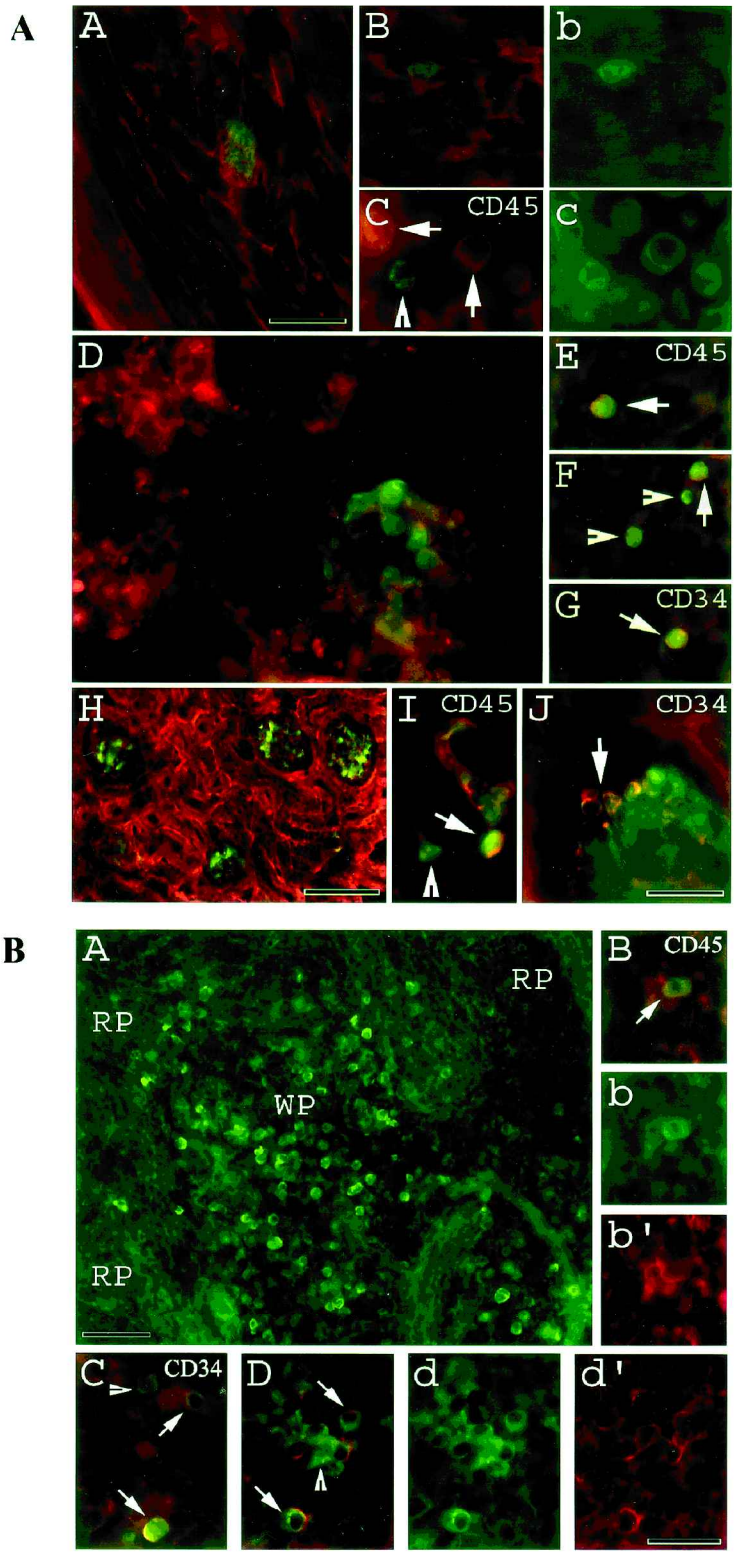
A
A
B
b
C
CD45
c
D
E
CD45
F
G
CD34
H
I
CD45
J
CD34
B
A
RP
RP
WP
RP
B
CD45
b
b'
C
CD34
D
d
d'

FIG. 4.

in the brain, cervical, and lumbar spinal cord. Immunophenotype(s) of transplanted cells were verified by double-staining for CD45, Nestin, TuJ1, and GFAP.

In the lumbar (Fig. 5A–D, panel A) and cervical spinal cord, targets of motor neuron degeneration in ALS, most cells congregated in, or some distance away from, the blood vessels and were immunoreactive for CD45. These hUCB cells outside the blood vessels did not express CD45 (Fig. 5D, panel A). Some of the administered cells were found in the parenchyma of the gray matter and expressed neural specific markers (Nestin, TuJ1, and GFAP). In Fig. 5, hUCB cells in a section of the lumbar spinal cord are shown expressing these markers. Using GFAP double-staining, we demonstrated that the hUCB cells were either surrounded by luminous astrocytes or themselves expressed this glial marker (Fig. 5E and F, panel A). Some transplanted cells were immunoreactive for Nestin and TuJ1 (Fig. 5G–J, panel A). Notably, administered hUCB cells in the cervical or lumbar spinal cord demonstrated several morphologically distinct cells typical of neuronal and glial cells (Fig. 5E,G,H,J, panel A). The HuNu-positive hUCB cells were also found in the lumbar central canal and in white matter of the cervical spinal cord.

As in the spinal cord, blood vessels in many structures of the brain contained hUCB cells (Figure 5A–C, panel B), which were immunoreactive for CD45 (Fig. 5A, panel B). Some cells were found within the brain parenchyma. Similar to cells expressing neural markers in the spinal cord, the hUCB cells in the brain were also immunopositive for Nestin, GFAP, and TuJ1 (Fig. 5F,H–J, panel B). Schematic distribution of hUCB cells within the brain is also shown in Fig. 6 for all expressing markers, including those in the blood vessels. Mainly, the administered hUCB cells expressing neural markers were found in the striatum, ventral tegmental area, corpus callosum, pons, frontal cortex, hippocampus, cerebellar lobules, ventromedial and ventrolateral thalamus, olfactory bulb, lateral olfactory tract, and the spinal trigeminal area. Interestingly, some cells in the brain parenchyma were also positive for CD45.

Thus, these results demonstrate that intravenously administered hUCB cells widely distribute not only in many organs, but also within the brain and spinal cord. The intraparenchymal migration of cells within the CNS showed that some cells can adopt neural phenotypes.

DISCUSSION

The major findings in our study were: (1) administration of the hUCB cells (10^6 cells) into the systemic circulation of G93A mice delays disease progression at least 2–3 weeks and increases the lifespan; (2) hUCB cells survive long-term (10–12 weeks) post-transplantation and enter regions of motor neuron degeneration in the brain and spinal cord; (3) hUCB cells migrate into the parenchyma of the brain and spinal cord and express early neural (Nestin), neuronal (TuJ1), and astrocytic (GFAP) markers; (4) hUCB cells are widely distributed in the peripheral organs (mainly, in the spleen) and some of these cells express CD34 antigen; (5) hUCB cells are present in the blood circuitry, possibly providing an additional cell supply.

Transplantation of hUCB, which is rich in hematopoietic progenitor/stem cells (22,23) and is being evaluated as an alternative to bone marrow, is capable of reconstituting blood cell lineages, and has been successfully used in pediatric clinics to treat various hematological malignant and nonmalignant diseases (36,37). Since 1988, when the first cord blood transplant was performed in a patient with Fanconi anemia (38), more than 2000 transplant cases have been reported worldwide (39). Recently, hUCB transplants from unrelated donors (vs. autologous

FIG. 5. Immunophenotypes of hUCB cells within the CNS after intravenous delivery. (**A**). Immunohistochemical staining of hUCB cells in the lumbar spinal cord. Parts A and B. Double-labeled HuNu/CD45 hUCB cells are found in or outside (part C) the blood vessels (HuNu, green; CD45, red/orange). (Part D) Some human (green) cells in parenchymal location were negative for CD45 and only stained with HuNu (green). (Part E) Double-labeled cells expressing GFAP (red) and HuNu (green) or surrounded by astrocytes (arrowhead) (part F). Part f is the same view as part F with fluorescein and rhodamine filters (part f′) to enhance green and red fluorescence, respectively. (Part G) Nestin expression (red) in double-labeled cell with HuNu (green). Stars indicate nuclei (DAPI) of mouse cells in tissue. Part g is the same view as part G with fluorescein and g′) rhodamine filters (part g′). (Parts H–J) Cells double-labeled for TuJ1 (red/orange, arrows) and HuNu (green). Part h is the same view as part H with fluorescein and rhodamine filters (part h′). The nuclei in part H are shown with DAPI and stars in parts H and h indicate the negative stain for TuJ1. Note: Nestin-positive and TuJ1–positive cells differ morphologically from any administered hUCB cells identified within the spinal cord. Scale bar: parts A–J, 25 μm. (**B**). Immunohistochemical staining of hUCB cells in the brain. Human cells were found in blood vessels (parts A–C) in many structures of the brain. They were: (part A) HuNu/CD45-positive (orange/red, double staining) or (parts B and C) only HuNu-positive (green). Some cells were found (part C) parenchymally at a distance from the blood vessel in corpus callosum (part D), ventral tegmental area (part E), pons (part F), frontal cortex (part G), olfactory bulb (part H), lateral olfactory tract (part I), and hippocampus (part J). The cells were also found in the striatum, cerebellar lobules, ventromedial thalamus, and spinal trigeminal area. Some cells were double stained with HuNu and GFAP (part F) or TuJ1 (H–J). The nuclei in parts H and J are shown with DAPI. Scale bar: parts A and C, 25 mm; part B, 50 mm.

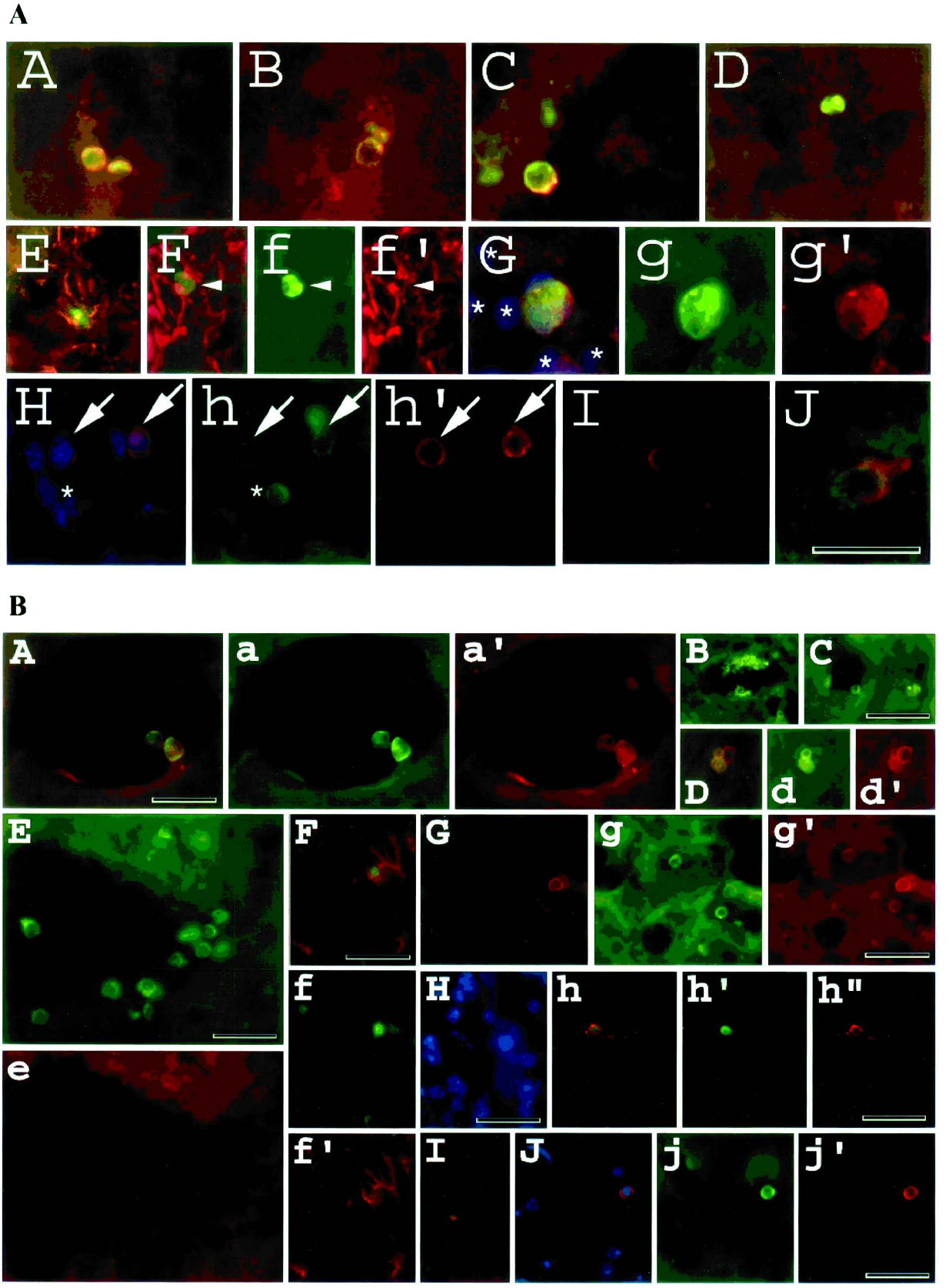

FIG. 5.

FIG. 6. Schematic distribution of hUCB cells in the brain of G93A mouse after intravenous administration. While some cells are found parenchymally, most cells associated with blood vessels express CD45. The hUCB cells expressing neural markers (Nestin, GFAP, and TuJ1) are found in the parenchyma, mainly in the striatum, ventral tegmental area, corpus callosum, pons, frontal cortex, hippocampus, cerebellar lobules, ventromedial and ventrolateral thalamus, olfactory bulb, lateral olfactory tract, and the spinal trigeminal area. The stars indicate distribution of cells within the brain, including those in the blood vessels. CA1, 3, Fields of hippocampus; DG, dentate gyrus; T, thalamus; LV, the lateral ventricle; cc, corpus callosum; CPu, caudate putamen; C, cerebellum; Fr, frontal cortex; Tu, olfactory tubercle; IC, inferior colliculus; ic, internal capsule; AA, anterior amygdaloid area; 4V, 4th ventricle; FN, facial nucleus; SpV, spinal trigeminal nucleus; SC, spinal cord. Magnification, 1.25×. Note: This 30-μm-thick sagittal section was cut on a cryostat.

transplantation) have shown promise as a treatment for children and adult patients (40–42).

A novel benefit of hUCB cells is that they can express antigens typical of neural lineages within the CNS. *In vitro* studies by our research group (24,25,28) and others (26,27) showed that hUCB-derived mononuclear cells cultured in standard growth (i.e., DMEM) or neuralization-inducing (RA + NGF) media, expressed specific markers for early neural precursors (Nestin, TuJ1), mature neurons (NeuN, MAP2), astrocytes (GFAP), and oligodendrocytes (GaLC). However, when hUCB cells were exposed to RA + NGF treatment, TuJ1 and GFAP expression increased by approximately two times (24). Similar to previous studies, we have demonstrated that DMEM-treated hUCB cells express neural markers, such as Nestin, TuJ1, MAP2, and GFAP. New findings in the present study are the co-localization of Nestin and MAP2 and various cytoplasmic locations of TuJ1 by cells at 2 weeks after plating—findings that we suggest may depend upon cell cycle or cell development. Additionally, the increased number of cells expressing CD133 antigen, a marker of primitive hematopoietic progenitor/stem cells, in 7 days cultured hUCB cells probably gives rise to cells which show immature and mature neural characteristics at the same time.

There is morphological and immunohistochemical evidence that hUCB can give rise to neural-like cells (24–28), so using these cells as an alternative cell source in the treatment of neurodegenerative disorders is an attractive approach. Recently, in a rat model of stroke, intravenous administration of hUCB cells (3×10^6) at 24 h or 7 days after middle cerebral artery occlusion significantly improved neurological function (29). Upon histological examination of the brains, hUCB cells were observed mainly in the cortex and striatum of the injured hemisphere in the ischemic boundary zone. Few cells were found in the contralateral hemisphere. Using immunohistochemistry, it was determined that some of these hUCB cells were immunoreactive for neuronal markers NeuN (2%) and MAP2 (3%), the astrocytic marker GFAP (6%), and the endothelial cell marker FVIII (8%). The hUCB cells were also detected outside the brain in bone marrow (3%), spleen (1%), muscle, heart, lung, and liver (0.01–0.5%). In another study, when hUCB cells (2×10^6) were delivered to the tail vein of rats with traumatic brain injury, neurological deficits were reduced (30). Wide distribution of administered cells in the brain and peripheral organs was detected. The cells, which migrated into the parenchyma of the injured brain, expressed neuronal markers NeuN and MAP2 and the astrocytic marker GFAP. Additionally, intravenously delivered hUCB (10^6), at 1 day or 5 days post-injury in

rats with compression injury of the spinal cord, increased the rate of behavioral recovery (31). However, rats that received the cells 1 day after injury showed significantly improved recovery of motor function compared to those that received cells on the 5th day post-injury, and both were significantly better than animals upon which only laminectomy was performed. Moreover, direct injection of hUCB-derived AC133 (hematopoietic progenitor/stem) cells into a demyelinated lesion of rat spinal cord showed extensive axon remyelination by light and electron microscopic examination (43). Thus, these studies demonstrated that hUCB cells delivered into the systemic circulation were able to migrate into injured/damaged areas of the brain or spinal cord and express neural-like markers without pre-exposure to specific factors. Although the mechanism of cell migration remains unclear, authors suggest that hUCB cells "may enter the brain from blood–brain barrier disruption or in response to signals from cytokines and cell surface receptors and antigens" and "the microenvironment of the brain after injury may drive hUCB cells into a neural cell phenotype" (30).

In the present study, we first demonstrated that hUCB cells, intravenously administered into a presymptomatic G93A SOD1 mouse model of ALS, delay disease progression by at least 2–3 weeks. The G93A mice typically lose 50% of their motor neurons in the cervical and lumbar spinal cord by 13 weeks of age, then hindlimb paralysis rapidly progresses (44–46), and death occurs at about 4–5 months of age. Our demonstration, that a low dose of hUCB administered to mice allows them to retain motor ability until 19 weeks of age, proves the effectiveness of this cell-based therapy. Although some transplanted cells survived long-term and expressed neuronal antigens within the CNS, questions remain about how these introduced neurons integrate into host tissue, as well as about how they grow and survive in the excitotoxic ALS environment. Also, it is naive to believe that hUCB cells develop into specific phenotypes due solely to external influences. Probably, interconnection and intercommunication between introduced and host cells occur by some combination of endo- and exogenous factors that may prompt hematopoietic stem cells to develop into a non-hematopoietic cell type. A future longitudinal study will attempt to answer some of these questions. The primary focus of the present study was a qualitative analysis of hUCB cells used in the possible treatment of ALS.

Supporting our working hypothesis about directed development of cells, we noted expression of CD34 antigens on hUCB cells in the spleen, liver, and kidneys. The CD34 antigen is a known membrane glycoprotein regulating the adhesion of stem cells to stromal cells (47). It is reasonable to suggest that, in the above organs, hUCB cells proliferated during the long-term post-transplant period, probably providing an additional cell supply. Another supporting finding was the distinct morphology of hUCB cells for each individual organ. Taking into account the higher proportion (0.98%) of progenitor/stem cells recently identified in nucleated cells of cord blood (48) compared to previous estimates (0.2–0.5%) (49), it is possible that stem cells can give rise to some cell types specific to the environment.

However, an important issue regarding the migration mechanism requires further discussion. One suggestion (see above) is that cell migration to lesioned areas of the brain or spinal cord occurs due to "signaling" substances in damaged tissues, substances that attract the transplanted cells. In ALS, in the brainstem and spinal cord of both patient and animal models, increasingly large numbers of activated microglia and astrocytes, immunoglobulin G (IgG), and T lymphocytes (50–53) may be capable of secreting the numerous cytokines playing key roles in the inflammatory reaction. The increase of macrophage-cytokines such as interleukin (IL)-1α, IL-1β, and IL-1RA (54), the proinflammatory enzyme cyclooxygenase type 2 (Cox-2) (51,55), and up-regulation of the tumor necrosis factor-α (TNF-α) gene (54,56) make them likely candidates for chemoattractants inducing cell migration. Interestingly, T cell-derived cytokines (lymphokines) including IL-2, IL-3, and IL-4 are not elevated in G93A mice, even at late stages of disease, which led to the suggestion that "lymphocyte contributions to cytokine expression in ALS are likely minor" (54). Other possible mechanisms of cell migration may involve natural monocyte diffusion or crossing of a damaged blood–brain barrier.

Additionally, if ALS is an autoimmune disease, as some have hypothesized (11–13,53,57), hUCB cells may improve disease outcome through immune modulation. Supporting this hypothesis is evidence showing that intravenous administration of a large dose (35×10^6) of hUCB cells into irradiated G93A mice substantially increased lifespan of mice (32). It has been shown that cord blood $CD34^+$ progenitor cells differentiate into $CD19^+$ B cell precursors after exposure to stem cell and granulocyte-stimulating factors. They are more immature than those derived from peripheral blood $CD34^+$ cells (58,59). The $CD25^+$ cells are also present in cord blood as 5% of $CD4^+$ T cells (60); they are naïve and might be regulatory T cells, converting to a memory T cell phenotype in adult blood. Thus, the immunomodulation of immune-effector changes in ALS by hUCB transplantation is possible but determining such is beyond the scope of this investigation. In our observations, many hUCB cells were present in white pulp of the spleen. From this "homing" of transplanted cells to the spleen, we suggest that behavioral improvements or increased lifespan may occur due to a peripheral immunological effect.

Stem cells derived from hUCB expressing substance P and its receptor (neurokinin-1) have been recently de-

scribed; substance P has an important role in immunomodulation of lymphocyte and monocyte/macrophage function (61). On the other hand, reduction of substance P binding has been noted in ALS patients, especially in the ventral horn associated with motor neuron degeneration (62). This loss of a trophic peptidergic neurotransmitter, as Barker suggests (63), may occur due to chronic autoimmune destruction following a viral infection of the central nervous system (CNS). So, the hUCB cells may have an additional trophic effect providing neuroprotective support to dying motor neurons.

Thus, results of our study indicate that hUCB may have therapeutic potential in the treatment of ALS by providing cell replacement and neuroprotection of motor neurons. Our novel findings demonstrate that after delivery of hUCB cells into the systemic circulation of SOD1 mice, cells may migrate to areas of motor neuron degeneration in the brain and spinal cord and adopt neural phenotypes, and are promising in the development of this noninvasive cell-based therapy for ALS. Furthermore, this is the first demonstration by our research group of systemically administered hematopoietic cells entering the brain and spinal cord in a noninjury disorder, which broadens the implications of this approach for other neurodegenerative diseases. Finally, cell replacement is probably not the main factor in the effectiveness of hUCB in this study due to the small number of cells expressing neural phenotypes. While we used a small dose of intravenously transplanted hUCB cells (10^6), increasing the cell dosage might further delay disease progression and increase lifespan of the SOD1 mice. Most likely, effectiveness of the hUCB cells is partially due to neuroprotection by modulation of the autoimmune process.

ACKNOWLEDGMENTS

This research was supported, in part, by Janet White Foundation for ALS Research, Inc., and the Children's Medical Research Foundation, Inc. We gratefully acknowledge the assistance of Nicole Kuzmin-Nichols for providing cells. We also acknowledge the assistance in behavioral experimentation and analysis by Blake Sowerby and Amber N. Cockburn. S. Garbuzova-Davis, A.E. Willing, T. Zigova, and S. Saporta are consultants to Saneron CCEL Therapeutics, Inc. PR Sanberg is a cofounder of Saneron-CCEL Therapeutics, Inc.

REFERENCES

1. McKay R. (1997). Stem cells in the central nervous system. Science 276:66–71.
2. Gage FH. (2000). Mammalian neural stem cells. Review. Science 287:1433–1438.
3. Bruijn LI. (2002). Amyotrophic lateral sclerosis: from disease mechanisms to therapies. BioTechniques 32:1112–11121.
4. Willing AE, S Garbuzova-Davis, S Saporta, M Milliken, DW Cahill and PR Sanberg. (2001). HNT neurons delay onset of motor deficit in a model of amyotrophic lateral sclerosis. Brain Res Bull 56:525–530.
5. Garbuzova-Davis S, AE Willing, M Milliken, S Saporta, T Zigova, DW Cahill and PR Sanberg. (2002). Positive effect of transplantation of hNT Neurons (Ntera 2/D1 cell-line) in a model of familial amyotrophic lateral sclerosis. Exp Neurol 174:169–180.
6. Garbuzova-Davis S, AE Willing, M Milliken, S Saporta, B Sowerby, DW Cahill and PR Sanberg. (2001). Intraspinal implantation of hNT neurons into SOD1 mice with apparent motor deficit. ALS and Other Motor Neuron Disorders 2:175–180.
7. Rothstein JD. (1996). Excitotoxicity hypothesis. Review. Neurology 47:19–25.
8. Shaw PJ and PG Ince. (1997). Glutamate excitotoxicity and amyotrophic lateral sclerosis. J Neurol 244:3–14.
9. Rosen DR, T Siddique T, D Patterson, DA Figlewicz, P Sapp, A Hentati, D Donaldson, J Goto, JP O'Regan, HX Deng, Z Rahmani, A Krizus, D McKenna-Yasek, A Cayabyab, SM Gaston, R Berger, RE Tanzi, JJ Halperin, B Herzfeld, R Van den Berg, WY Hung, T Birg, G Deng, DW Mulder, C Smyth, NG Laing, E Soriano, MA Perciak-Vance, J Haines, GA Roulou, JS Gusella, HR Horvitz and RH Brown Jr. (1993). Mutations in Cu/Zn superoxide dismutase gene are associated with familial Amyotrophic lateral sclerosis. Nature 362:59–62.
10. Berger MM, N Kopp, C Vital, B Redl, M Aymard and B Lina. (2000). Detection and cellular localization of enterovirus RNA sequences in spinal cord of patients with ALS. Neurology 54:20–25.
11. Niebroj-Dobosz I, A Jamrozik, P Janik, I Hausmanowa-Petrusewicz and H Kwiecinski. (1999). Anti-neural antibodies in serum and cerebrospinal fluid of amyotrophic lateral sclerosis (ALS) patients. Acta Neurol Scand 100:238–243.
12. Alexianu ME. (1995). The role of immune processes in amyotrophic lateral sclerosis pathogenesis. Rom J Neurol Psychiatry 33:215–227.
13. Appel SH, RG Smith, ME Alexianu, JI Engelhardt and E Stefani. (1995). Autoimmunity as an etiological factor in sporadic amyotrophic lateral sclerosis. Review. Adv Neurol 68:47–57.
14. Warita H, Y Itoyama and K Abe. (1999). Selective impairment of fast anterograde axonal transport in the peripheral nerves of asymptomatic transgenic mice with a G93A mutant SOD1 gene. Brain Res 819:120–131.
15. Beaulieu JM, H Jacomy and JP Julien. (2000). Formation of intermediate filament protein aggregates with disparate effects in two transgenic mouse models lacking the neurofilament light subunit. J Neurosci 20:5321–5328.
16. Migheli A, S Cordera, C Bendotti, C Atzori, R Piva and D Schiffer. (1999). S-100 beta protein is upregulated in astrocytes and motor neurons in the spinal cord of patients with amyotrophic lateral sclerosis. Neurosci Lett 261:25–28.
17. Cho KJ, YH Chung, C Shin, DH Shin, YS Kim, ME Gurney, KW Lee and CI Cha. (1999). Reactive astrocytes ex-

press p53 in the spinal cord of transgenic mice expressing a human Cu/Zn SOD mutation. NeuroReport 10:3939–3943.
18. Levine JB, J Kong, M Nadler and Z Xu. (1999). Astrocytes interact intimately with degenerating motor neurons in mouse amyotrophic lateral sclerosis (ALS). Glia 28: 215–224.
19. Hall ED, J Oostveen and ME Gurney. (1998). Relationship of microglial and astrocytic activation to disease onset and progression in a transgenic model of familial ALS. Glia 23:249–256.
20. Sasaki S and M Iwata. (1996). Ultrastructural study of synapses in the anterior horn neurons of patients with amyotrophic lateral sclerosis. Neurosci Lett 204:53–56.
21. Menzies FM, PG Ince and PJ Shaw. (2002). Mitochondrial involvement in amyotrophic lateral sclerosis. Neurochem Int 40:543–551.
22. Mayany H and PM Lansdorp. (1998). Biology of human umbilical cord blood-derived hematopoietic stem/progenitor cells. Stem Cells 16:153–165.
23. Todaro AM, C Pafumi, G Pernicine, S Munda, MR Pilastro, A Russo, M Farina and A Messing. (2000). Haematopoietic progenitors from umbilical cord blood. Blood Purif 18:144–147.
24. Sanchez-Ramos JR, S Song, SG Kamath, T Zigova, A Willing, F Cardozo-Petaez, T Stedeford and M Chopp. (2001). Expression of neural markers in human umbilical cord blood. Exp Neurol 171:109–115.
25. Sanchez-Ramos JR. (2002). Neural cells derived from adult bone marrow and umbilical cord blood. J Neurosci Res 69:880–893.
26. Bicknese AR, HS Goodwin, CO Quinn and CD Verneake. (2002). Human umbilical cord blood cells can be induced to express markers for neurons and glia. Cell Transplant 11:261–264.
27. Ha Y, JU Choi, DH Yoon, DS Veon, JJ Lee, HO Kim and YE Cho. (2001). Neural phenotype expression of cultured human cord blood cells *in vitro.* NeuroReport 12:3523–3527.
28. Zigova T, S Song S, AE Willing, JE Hudson, MB Newman, S Saporta, J Sanchez-Ramos and PR Sanberg. (2002). Human umbilical cord blood cells express neural antigens after transplantation into the developing rat brain. Cell Transplant 11:265–274.
29. Chen J, PR Sanberg, Y Li, L Wang, M Lu, AE Willing, J Sanchez-Ramos and M Chopp. (2001). Intravenous administration of human umbilical cord blood reduces behavioral deficit after stroke in rats. Stroke 32: 2682–2688.
30. Lu D, PR Sanberg, A Mahmood, Y Li, L Wang, R Sanchez-Ramos and M Chopp. (2002). Intravenous administration of human umbilical cord blood reduces neurological deficit in the rat after traumatic brain injury. Cell Transplant 11:275–285.
31. Kim JJ, S Saporta, AE Willing, ES Fu, LO Colina and PR Sanberg. (2002). Behavioral recovery following intravenous administration of human umbilical cord blood cells in rats with spinal cord injury. Exp Neurol 175:443.
32. Ende N, F Weistein, R Chen and M Ende. (2000). Human umbilical cord blood effect on SOD mice (amyotrophic lateral sclerosis). Life Sci 67:53–59.
33. Chen R and N Ende. (2000). The potential for the use of mononuclear cells from human umbilical cord blood in the treatment of amyotrophic lateral sclerosis in SOD1 mice. J Med 31:21–30.
34. Gurney ME, H Pu, AY Chiu, C Dal Canto, CY Polchow, DD Alexander, J Caliendo, A Hentati, YW Kwon, HX Deng, W Chern, P Zhai, RW Sufit and T Siddique. (1994). Motor neuron degeneration in mice that express a human Cu/Zn superoxide dismutase mutation. Science 264:1772–1775.
35. Mason MRJ, G Campbell, P Caroni, PN Anderson and AR Lieberman. (2000). Overexpression of GAP-43 in thalamic projection neurons of transgenic mice does not enable them to regenerate axons through peripheral nerve grafts. Exp Neurol 165:143–152.
36. Lu M, RN Shen and HE Broxmeyer. (1996). Stem cells from bone marrow, umbilical cord blood and peripheral blood for clinical application: current status and future application. Crit Rev Oncol Hematol 22:61–78.
37. Sirchia G and P Rebulla. (1999). Placental/umbilical cord blood transplantation. Review. Haematologica 84:738–747.
38. Gluckman E, HE Broxmeyer, AD Auerbach, HS Friedman, GW Douglas, A Devergie, H Esperou, D Thierry D, G Socie, P Lehn et al. (1989). Hematopoietic reconstitution in a patient with Fanconi's anemia by means of umbilical cord blood from an HLA-identical sibling. N Engl J Med 321:1174–1178.
39. Gluckman E. (2000). Current status of umbilical cord blood hematopoietic stem cell transplantation. Exp Hematol 28: 1197–1205.
40. Rubinstein P, C Carrier, A Scaradavou, J Kurtzberg, J Adamson, AR Migliaccio, RL Berkowitz, M Cabbad, NL Dobrila, PE Taylor, RE Rosenfield and CE Stevens. (1998). Outcomes among 562 recipients of placental blood transplants from unrelated donors. N Engl J Med 339:1565–1577.
41. Wagner JE, JN Barker, TE DeFor, KS Baker, BR Blazar, C Eide, A Goldman, J Kersey, W Krivit, ML MacMillan, PJ Orchard, C Peters, DJ Weisdorf, NKC Ramsay and SM Davies. (2002). Transplantation of unrelated donor umbilical cord blood in 102 patients with malignant and nonmalignant diseases: influence of CD34 cell dose and HLA disparity on treatment-related mortality and survival. Blood 100:1611–1618.
42. Ooi J, T Iseki, S Takahashi, A Tomonari, H Nagayama, K Ishii, K Ito, H Sato, T Takahashi, M Shindo, R Sekine, N Ohno, K Uchimaru, F Nagamura, N Shirafuji, A Tojo, K Tani and S Asano. (2002). A clinical comparison of unrelated cord blood transplantation and unrelated bone marrow transplantation for adult patients with acute leukaemia in complete remission. Br J Haematol 118:140–143.
43. Honmou O, S Oka, K Houkin, K Hashi and JD Kocsis. (2002). AC133-positive cells derived from human cord blood remyelinate demyelinated axons in the adult rat spinal cord. Program No. 34.2, 2002 Abstracts Viewer/Itinerary Planner. Washington DC: Society for Neuroscience. CD-ROM.
44. Chiu AY, P Zhai, MC Dal Canto, TM Peters, YW Kwon, SM Prattis and ME Gurney. (1995). Age-dependent penetrance of disease in a transgenic mouse model of familial amyotrophic lateral sclerosis. Mol Cell Neurosci 6:349–362.
45. Azzouz M, N Leclerc, M Gurney, JM Warter, P Poindron and J Borg. (1997). Progressive motor neuron impairment

in an animal model of familial amyotrophic lateral sclerosis. Muscle Nerve 20:45–51.
46. Barneoud P, J Lolivier, DJ Sanger, B Scatton and P Moser. (1997). Quantitative motor assessment in FALS mice: a longitudinal study. NeuroReport 8:2861–2865.
47. Sutherland DR and A Keating. (1992). The CD34 antigen: structure, biology and potential clinical application. J Hematother 1:115–129.
48. Nayar B, GMK Raju and D Deka. (2002). Hematopoietic stem/progenitor cell harvesting from umbilical cord blood. Int J Gynecol Obstetr 79:31–32.
49. Killinburgh D and NH Russel. (1993). Comparative study of CD34 positive cells and subpopulations in human umbilical cord blood and bone-marrow. Bone Marrow Transpl 12:489–494.
50. Hall ED, JOA Oostveen and ME Gurney. (1998). Relationship of microglial and astrocytic activation to disease onset and progression in a transgenic model of familial ALS. Glia 23:249–256.
51. McGeer PL and EG McGeer. (2002). Inflammatory processes in amyotrophic lateral sclerosis. Muscle Nerve 26:459–470.
52. Elliot JL. (2001). Cytokine upregulation in a murine model of familial amyotrophic lateral sclerosis. Brain Res Mol Res 95:172–178.
53. Alexianu ME, M Kozovska and SH Appel. (2001). Immune reactivity in a mouse model of familial ALS correlates with disease progression. Neurology 57:1282–1289.
54. Hensley K, RA Floyd, B Gordon, S Mou, QN Pye, C Stewart, M West and K Williamson. (2002). Temporal patterns of cytokine and apoptosis-related gene expression in spinal cords of the G93A-SOD1 mouse model of amyotrophic lateral sclerosis. J Neurochem 82:365–374.
55. Almer G, C Guegan, P Teismann, A Naini, G Rosoklija, AP Hays, C Chen and S Przedborski. (2001). Increased expression of the pro-inflammatory enzyme cyclooxygenase-2 in amyotrophic lateral sclerosis. Ann Neurol 49:176–185.
56. Yoshihara T, S Ishigaki, M Yamamoto, Y Liang, J Niwa, H Takeuchi, M Doyu and G Sobue. (2002). Differential expression of inflammation- and apoptosis-related genes in spinal cords of a mutant SOD1 transgenic mouse model of familial amyotrophic lateral sclerosis. J Neurochem 80: 158–167.
57. Kawamata T, H Akiyama, T Yamada and PL McGeer. (1992). Immunologic reactions in amyotrophic lateral sclerosis brain and spinal cord tissue. Am J Pathol 140:691–707.
58. Hirose Y, H Kiyoi, K Iton, K Kato, H Saito and T Naoe. (2001). B-cell precursors differentiated from cord blood CD34+ cells are more immature than those derived from granulocyte colony-stimulating factor-mobilized peripheral blood $CD34^+$ cells. Immunology 104:410–417.
59. Ohkawara JI, K Ikebuchi, M Fujihara, N Sato, F Hirayama, M Yamaguchi, KJ Mori and S Sekiguchi. (1998). Culture system for extensive production of $CD19^+$ IgM^+ cells by human cord blood $CD34^+$ progenitors. Leukemia 12:764–771.
60. Wing K, A Ekmark, H Karlsso, A Rudin and E Suri-Payer. (2002). Characterization of human $CD25^+CD4^+$ T cells in thymus, cord and adult blood. Immunology 106:190–199.
61. Li Y, SD Douglas and W Ho. (2000). Human stem cells express substance P gene and its receptor. J Hematother Stem Cell Res 9:445–452.
62. Dietl MM, M Sanchez, A Probst and JM Palacios. (1989). Substance P receptors in the human spinal cord: decrease in amyotrophic lateral sclerosis. Brain Res 483:39–49.
63. Barker R. (1991). Substance P and neurodegenerative disorders. A speculative review. Neuropeptides 20:73–78.

Address reprint requests to:
Dr. Paul P. Sanberg
Center for Aging and Brain Repair
Department of Neurosurgery
University of South Florida, College of Medicine
12901 Bruce B. Downs Boulevard, MDC 78
Tampa, FL 33612

E-mail: psanberg@hsc.usf.edu

Received March 10, 2003; accepted April 5, 2003.